

Elsevier required licence: © <2021>. This manuscript version is made available under the CC-BY-NC-ND 4.0 license <http://creativecommons.org/licenses/by-nc-nd/4.0/>
The definitive publisher version is available online at
[\[https://www.sciencedirect.com/science/article/pii/S2352186421001565?via%3Dihub\]](https://www.sciencedirect.com/science/article/pii/S2352186421001565?via%3Dihub)

1 **Proof of concept: Integrated membrane distillation-forward**
2 **osmosis approaches water production in a low-temperature**
3 **CO₂ capture**

4 Manuscript submitted to

5 *Environmental Technology & Innovation*

6 Lei Zheng ^{1,2}, Kangkang Li ³, Qilin Wang ¹, Gayathri Naidu ¹, William E. Price ⁴, Xiwang Zhang
7 ⁵, and Long D. Nghiem ^{1,6,*}

8
9
10
11 ¹ Centre for Technology in Water and Wastewater, University of Technology Sydney, Ultimo
12 NSW 2007, Australia

13 ² Chongqing Institute of Green and Intelligent Technology, Chinese Academy of Sciences,
14 Chongqing 400714, PR China

15 ³ CSIRO Energy, 10 Murray Dwyer Circuit, Mayfield West, NSW 2307, Australia

16 ⁴ Strategic Water Infrastructure Laboratory, School of Chemistry and Molecular Biosciences,
17 University of Wollongong, NSW 2522, Australia

18 ⁵ Department of Chemical Engineering, Monash University, Clayton, VIC 3800, Australia

19 ⁶ NTT Institute of Hi-Technology, Nguyen Tat Thanh University, Ho Chi Minh City, Vietnam

20 * Corresponding author: Long D. Nghiem. Email: Duclong.Nghiem@uts.edu.au; Ph +61 2 9514
21 2625

22 **Abstract**

23 This study investigated the removal of CO₂ from flue gas by an integrated membrane distillation-
24 forward osmosis (MD-FO) system. Monoethanolamine (MEA) and sodium glycinate solutions
25 were loaded with CO₂ from a mixture of CO₂ and N₂ (1:9 in volume ratio) to simulate synthetic
26 flue gas. CO₂ desorption from the amine solution was evaluated using MD at 80 °C. Interaction
27 between amines and the membrane polymeric matrix could alter the membrane surface
28 hydrophobicity; however, under all experimental conditions it was still sufficiently hydrophobic
29 for MD operation. Amine loss during MD operation for CO₂ desorption was insignificant. FO was
30 used to provide make-up water and cooling to the regenerated amine solution after CO₂ desorption
31 by MD. The results showed stable FO water flux when wastewater effluent was used as the source
32 for make-up water. Repetitive CO₂ loading and desorption experiments showed 87.0% and 88.1%
33 CO₂ re-absorption efficiency for MEA and sodium glycinate in the second cycle, respectively.
34 Further investigation of this hybrid system is suggested to advance the CO₂ desorption by MD
35 process and water production by FO process.

36 **Keywords:** CO₂ capture; Flue gas; Membrane distillation; Forward osmosis; Monoethanolamine;
37 Sodium glycinate.

38 **1 Introduction**

39 CO₂ removal from flue gas for storage or beneficial utilisation is a pragmatic solution while
40 non fossil-based energy alternatives are still being developed. Fossil fuel combustion produced
41 37.15 Gt of CO₂, equivalent to 45% of the global green house gas emission [1]. To reduce
42 green house gas emission from the combustion of fossil fuel, strategies for CO₂ capture from
43 flue gas such as absorption [2], membrane separation [3-5] and adsorption [6-8] have been
44 extensively studied in recent years. Amine-based post-combustion CO₂ capture is a mature
45 technology that can be retrofitted to existing power stations. Examples of power stations
46 retrofitted with amine-based post-combustion CO₂ capture include Boundary Dam [9] and
47 Petra Nova [10].

48 Monoethanolamine (MEA) is the most widely used chemical for amine-based CO₂ capture due
49 to features such as high absorption capacity, fast reaction kinetics and high mass transfer. Apart
50 from MEA, several amino acid salts such as sodium glycinate have also gained scientific and
51 commercial attention because of their greater resistances to oxidative degradation and lower
52 toxicity than MEA [11, 12]. These amino acid salts have an amine group and an acidic
53 carboxylic acid group, which can be protonated, neutral, or deprotonated as a function of pH
54 [13]. The zwitterionic mechanism is often considered to interpret the chemical reaction
55 between CO₂ and solvents [14, 15]. In this mechanism, a primary or secondary amino group of
56 amines firstly reacts with CO₂ to form a zwitterion (Eq. 1). The base (i.e. amine, OH⁻, or H₂O)
57 neutralizes the intermediate to form a carbamate (Eq. 2). These carbamates can be thermally
58 reversed back to amine and CO₂ via the following reactions:



61 In the current amine-based CO₂ removal process, amine solution is regenerated by a stripping
62 with steam at about 120 °C. This thermal energy consumption accounts for about 75% of the
63 overall costs because of large amount of steam used for the absorbent regeneration [16-18]. In
64 addition, the high stripping temperature resulted in thermal degradation and subsequent amine
65 loss [19]. Recent approaches to address these drawbacks focus on the absorbent formulation
66 and process innovation to improve the CO₂ capture performance, such as solvent modification
67 with promoters, efficient gas-liquid contactors, microwave swing regeneration and,
68 electrochemically mediated amine regeneration [20-22]. For example, Li et al, [23, 24]
69 observed that addition of metal ions (i.e. Cu and Me) in the aqueous amine solution could

70 enhance the CO₂ desorption rate and reduce the heat of CO₂ desorption, thus reducing the
71 regeneration energy. However, these approaches still rely on high temperature CO₂ desorption,
72 and have not been realised at full scale for CO₂ capture. Another inherent disadvantage of high
73 temperature CO₂ desorption is the high energy demand for cooling. The large water demand
74 for the trim cooler is a major hurdle for inland CO₂ capture plants where fresh water is scarce.

75 New research effort has been devoted to technologies with low CO₂ desorption temperature so
76 that the low-grade waste heat from the power plants can be utilised. In the US alone, thermal
77 power plants discharge 18.9 billion GJ_{th} waste heat each year at temperature around 85 °C [25].
78 If fully utilised this waste heat can offset most of the thermal energy requirement for CO₂
79 capture.

80 The CO₂ desorption kinetics from an amine solution is slow. However, the rate of CO₂
81 desorption can be improved by removing or reducing water activities in the system. Lin et al.,
82 [26] lowered the water activity by adding methanol into a water-amine system and observed
83 67% higher CO₂ desorption at 80 °C than that of MEA only at 120 °C in terms of the cyclic
84 loading performance. Lai et al., [27] also observed higher CO₂ desorption rate in an alcohol-
85 amine-water system than that of a single amine system. In the 40 wt% ethanol/20 wt% MEA
86 solution, CO₂ desorption rate was reported to increase by more than 6 times, from 0.021 to
87 0.137 mmol/s. This may be attributed to dielectric constant compression of amine due to
88 alcohol addition and therefore reduced the basic strength of the sorbent, which helped to release
89 acidic CO₂ at a low temperature [28]. Barzagli et al., [29, 30] reported that MEA was more
90 stable than other secondary amines (e.g. amines 2-2(2-aminoethoxy)ethanol) with more
91 residual carbamates at 110 °C desorption by ¹³C NMR spectroscopy. They also observed that
92 a mixture of amines (i.e. alkanolamine and 2-amino-2-methyl-1-propanol) could achieve 73-
93 96% efficiency at the low desorption temperature (< 90 °C). Another approach is to remove
94 water from the system during CO₂ desorption, which can also increase CO₂ desorption rate.

95 Membrane distillation (MD) can utilise low-grade heat and remove water at the same time,
96 enabling MD a good candidate for the low temperature CO₂ desorption. Unlike pressure driven
97 membrane technologies (such as nanofiltration and reverse osmosis), MD is a thermally driven
98 separation process. The difference in partial water vapour pressure across a microporous and
99 hydrophobic membrane induced by temperature difference between the feed and distillate side
100 is the driving force of the MD process [31, 32]. The membrane surface properties can be
101 precisely controlled to achieve anti-fouling and anti-wetting properties [33-35].

102 MD is operated at well below the water boiling temperature. Thus, the low-grade heat from
103 power plants can be directly utilised in MD process to regenerate the amine solution after heat
104 exchanger at 80 °C or below. MD can remove water from the water-amine solution to improve
105 the rate of CO₂ desorption. MD has been successfully demonstrated at pilot scale for further
106 removal of water from hypersaline solutions [36, 37]. Several studies have also demonstrated
107 the potential of low-temperature CO₂ desorption from amine and amino acid salt by hollow
108 fibre membrane contactors [21, 38, 39]. However, to date, the feasibility of MD for low-
109 temperature (~80 °C) CO₂ desorption has not been systematically investigated.

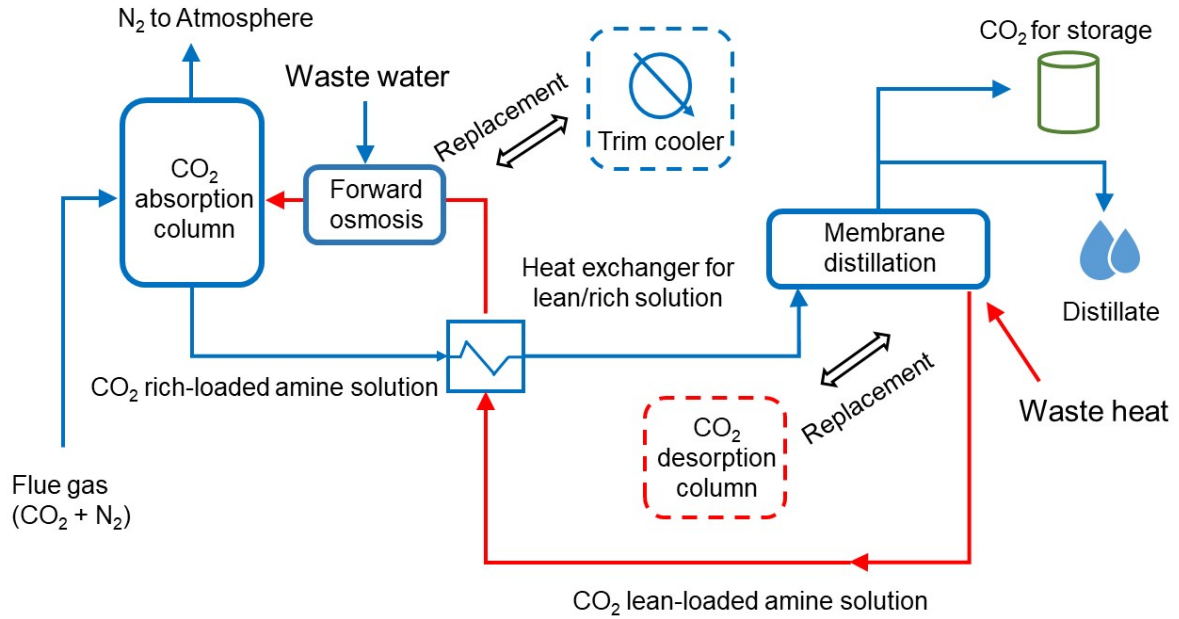
110 In the amine-based CO₂ capture process, after regeneration, it is necessary to cool down the
111 amine solution to a desired CO₂ absorption temperature and compensate to the corresponding
112 water loss from the CO₂ desorption. Previous studies [40-42] have demonstrated the potential
113 of forward osmosis (FO) for simultaneous cooling of the regenerated amine solution and
114 providing make-up water.

115 In this study, we propose an integrated MD-FO system to simultaneously achieve two
116 objectives: (1) CO₂ desorption at low temperature; (2) cooling and provision of make-up water
117 after desorption. This study aims to extend the previous theoretical framework and to evaluate
118 the effect of membrane material and adsorbent type on the system performance.

119 **2 Materials and methods**

120 **2.1 Conceptual diagram of proposed MD-FO for CO₂ capture**

121 Fig. 1 conceptually describes the proposed MD-FO process for low temperature CO₂ capturing
122 from flue gas. Inputs into the process are flue gas and waste heat from coal fired power plants
123 and wastewater. Outputs from the process include purified CO₂ for storage or beneficial use,
124 high quality distillate, and N₂ that can be vented to the atmosphere. Via an adsorption-
125 desorption cycle, pure CO₂ is extracted from flue gas for compression, storage or beneficial
126 use. Wastewater is used as the make-up water via the FO process. Waste heat from the power
127 plant is used to desorb CO₂ (regenerate the amine solution) and produce high quality distillate
128 for beneficial use.



129

130 Fig. 1. Conceptual integrated MD-FO process flow diagram. The process includes two stages:
 131 (1) CO₂ desorption supplement by membrane distillation for low temperature operation; and
 132 (2) Forward osmosis to replace a trim cooler.

133 2.2 Membranes and chemicals

134 Two commercially available flat-sheet hydrophobic polytetrafluoroethylene (PTFE)
 135 membranes were used for the MD process (Table 1). A flat-sheet hydrophilic thin film
 136 composite (TFC) membrane (Porifera, US) was used for FO process. This TFC membrane
 137 consists of a thin active layer and an embedded woven support layer. The operational ranges
 138 of pH of these membranes are between 3 and 13, which cover the pH range of the amine
 139 solution before and after CO₂ absorption.

140 Table 1: Specifications of hydrophobic membranes used in this study.

Membrane	Supplier	Thickness (μm)	Porosity (%)	Pore size (μm)
1	General Electric (US)	179	75	0.22
2	Porous Membrane Technology (China)	60	80	0.2

141 Reagent grade MEA, glycine and sodium hydroxide were from Sigma-Aldrich. Sodium
 142 glycinate was prepared by mixing glycine with an equal molar ratio between glycine and
 143 sodium hydroxide in deionised (DI) water. Instrument grade (>99.8% purity) CO₂ and N₂ gases
 144 were from Coregas Australia and stored in pressurised cylinders.

145 2.3 Feed solution for MD and FO

146 CO₂ and N₂ gases were mixed together using Bronkhorst mass flow controllers to obtain a
147 CO₂:N₂ gas ratio by volume of 1:9 to simulate the composition of flue gas. Simulated flue gas
148 was constantly bubbled into the 5 L of MEA (5 M) or sodium glycinate (3 M) solution at a
149 flow rate of 1.1 L/min at 40 °C controlled by a water bath. Gaseous CO₂ concentration was
150 analysed by a gas analyser (Horiba, VA-3000) with the analytical range of 0-10 vol% every 15
151 s. The CO₂ rich solution was considered fully loaded when CO₂ concentration in the outlet was
152 the same as in the inlet. These CO₂ rich-loaded solutions were used as the feed solution for MD
153 experiment.

154 CO₂ rich-loaded solutions became CO₂ lean-loaded solution after CO₂ desorption in the MD
155 experiment and CO₂ lean-loaded solutions were used as the draw solution in FO process. As a
156 kind of non-portable water, treated effluent from a membrane bioreactor [43] was used as the
157 feed solution in FO process. The conductivity and total organic carbon (TOC) of this treated
158 effluent was 5 mS/cm and 7 mg/L. DI water was used as the feed solution in the baseline test
159 with the same draw solution for treated effluent.

160 2.4 MD for CO₂ desorption and FO for water supplement

161 The CO₂ desorption experiments for CO₂ rich-loaded solution were performed using a lab-
162 scale direct contact membrane distillation (DCMD) system (Supplementary Data Fig. S1a).
163 The membrane module was in a plate-and-frame configuration with an effective membrane
164 area of 17.5 cm². Feed solution (0.5 L) and distillate (2 L) were circulated counter-currently by
165 two gear pumps (Cole Parmer, model 75211-15, US) at the flow rate of 1.0 L/min
166 (corresponding to 36.2 cm/s). In all experiments, the CO₂ rich-loaded feed solution was placed
167 in a jacketed vessel coupled with a temperature control system (Thermoline, model BL-30,
168 Australia) and maintained at 80 ± 2 °C. 80 °C represents the low-grade power plant waste heat
169 [44], which is a reasonably low temperature compared to the conventional regeneration
170 temperature (120 °C). The distillate was maintained at room temperature (25 ± 2 °C) using
171 another temperature control system (Thermoline, model BL-30, Australia). Inlet and outlet
172 temperature of the feed solution and distillate flow channels were recorded by temperature
173 sensors (Vernier LabQuest 2, US).

174 The distillate reservoir vessel was placed on a digital balance (Adam, model PGL 8001,
175 Australia) and the weight change was recorded every 3 min and transferred to a data logger.
176 Preliminary experiments showed that CO₂ desorption stopped at water recovery of 30% or
177 more. Samples (2 mL) from the feed solution were collected at 10, 20, and 30% water recovery

178 to monitor the CO₂ desorption performance as a function of water recovery. Feed and distillate
179 samples (50 mL) were also taken at the beginning and end of each experiment for other analyses.
180 Upon the DCMD process, the final concentrated feed solutions were then used as draw
181 solutions for the subsequent FO experiments.

182 After the CO₂ desorption experiment, the experimental equipment was rearranged into an FO
183 system. The same membrane cell was used for the FO system to provide make-up water and
184 cooling to the CO₂ lean-loaded solution also known as the regenerated amine solution
185 (Supplementary Data Fig. S1b). Draw solution (0.35 L) and feed solution (2 L) were circulated
186 counter-currently. The feed solution reservoir was placed on the digital balance for monitoring
187 the water flux. It is assumed that amine loss during CO₂ desorption did not occur. Thus, each
188 experiment was conducted until the amine solution returned to the initial volume of 0.5 L prior
189 to CO₂ desorption. In other words, the volume of water permeated through the membrane to
190 the CO₂ lean-loaded solution was the same as the volume of clean water produced by MD
191 during CO₂ desorption. Feed solution and draw solution samples (50 mL) were taken at the
192 beginning and end of each experiment for analysis. All DCMD and FO experiments were
193 conducted in duplicate. The results are reported as geometric mean and standard deviation.

194 2.5 Measurement and analysis

195 2.5.1 Contact angle measurement

196 Membrane surface hydrophobicity was determined by contact angle measurement using a
197 goniometer (model: Theta Lite 100, Biolin Scientific, Sweden) and the standard sessile drop
198 method. Five measurements using DI water (5-8 μ L) as the reference liquid were conducted at
199 different locations on the membrane surface. Membrane samples were air-dried before contact
200 angle measurement.

201 2.5.2 Solution chemistry characterization

202 The chemical properties of the liquid sample (1 μ L) were analysed by using a Fourier transform
203 infrared (FTIR) spectroscopy (model: IRAffinity-1, Shimadzu, Japan) equipped with a single
204 reflection attenuated total reflectance (MIRacle 10, Shimadzu, Japan). Absorbance from
205 wavelength 400 to 4000 cm^{-1} of each sample displayed the corresponding spectra at 4 cm^{-1}
206 resolution. TOC analysis was operated by sparging Non-Purgeable Organic Carbon using a
207 TOC analyser (Analytik Jena Multi N/C 3100, Jena, Germany).

208 2.5.3 Water flux and reverse salt flux

209 Water flux (J_w) is an important performance indicator of membrane process, which can be
210 calculated as follow:

$$211 \quad J_w = \frac{M_{t1} - M_{t2}}{\Delta t \times A \times \rho} \quad (1)$$

212 where M_{t1} and M_{t2} are the weights of distillate (MD)/feed solution (FO) at time $t1$ and $t2$,
213 respectively. Δt is the time interval (3 min); A is the effective membrane area; and ρ is water
214 density.

215 Due to the constant ratio of carbon for MEA and sodium glycinate, it was possible to carry out
216 TOC analysis to analyse their respective concentration in the solution sample. Reverse salt flux
217 (J_s) indicates the mass diffusion from draw solution to feed solution, which can be calculated
218 based on the mass balance calculation as follow:

$$219 \quad J_s = \frac{(C_t \times V_{feed,t} - C_0 \times V_{feed,0})}{A \times t} \quad (2)$$

$$220 \quad V_{feed,t} = V_{feed,0} - \Delta V_{p,t} \quad (3)$$

221 where $V_{feed,0}$ and $V_{feed,t}$ are the volumes of the feed at the beginning and corresponding time t
222 of the experiment; C_0 and C_t are the concentrations of draw solution in the feed at the beginning
223 and corresponding time t of the experiment, respectively; $\Delta V_{p,t}$ is the volume of distillate at
224 time t . The solute rejection by MD is calculated based on dilution factor ($DF = V_{draw}/\Delta V_{p,t}$) as
225 follow:

$$226 \quad R(\%) = \left(1 - \frac{DF \times C_{distillate}}{C_{feed}} \right) \times 100 \quad (4)$$

227 Water recovery (R_w) of MD/FO experiment is defined as the volume fraction of feed that is
228 recovered as permeate:

$$229 \quad R_w = \frac{Q_p}{Q_F} \quad (5)$$

230 where Q_p represents the volume of water production, Q_F denotes the volume of feed.

231 2.5.4 CO₂ loading ratio analysis

232 The CO₂ loading ratio (α , mol of CO₂/mol of amine) values after absorption and desorption
233 were determined by the excessive acid method [45]. By adding an excess amount of strong acid

234 (i.e. 2 mol/L H₂SO₄) to the liquid sample, CO₂ in the liquid sample was released into the gas
235 phase and precisely measured by the variable volume in a burette.

$$236 \quad \alpha = \frac{V_{CO_2}}{22.4 \times V_L \times m} \times \frac{P}{P_0} \times \frac{273}{t} \quad (6)$$

237 where V_{CO₂} denotes the measured volume of released CO₂ from the sample, mL; V_L represents
238 sample volume, mL; m denotes the molar concentration of sample, mol/L; P/P₀ stands for the
239 ratio between room atmospheric pressure and standard atmospheric pressure; t is the room
240 temperature, K. In addition, the accuracy of this method was validated by using different
241 concentrations of sodium carbonate (0.5, 1, and 2 M) aqueous solutions.

242 The CO₂ desorption efficiency, ρ, is obtained by the following equation:

$$243 \quad \rho(\%) = \left(1 - \frac{\alpha_f}{\alpha_i}\right) \times 100 \quad (7)$$

244 where α_i and α_f represent initial and final loading of CO₂ rich-loaded and lean-loaded amine
245 solutions. On the other hand, CO₂ re-absorption efficiency, η, is used to compare the loading
246 of CO₂ re-absorption solution (α_r) to that of initial CO₂ rich-loaded solution (α_i).

$$247 \quad \eta(\%) = \frac{\alpha_r}{\alpha_i} \times 100 \quad (8)$$

248 **3 Results and discussions**

249 **3.1 DCMD for CO₂ desorption**

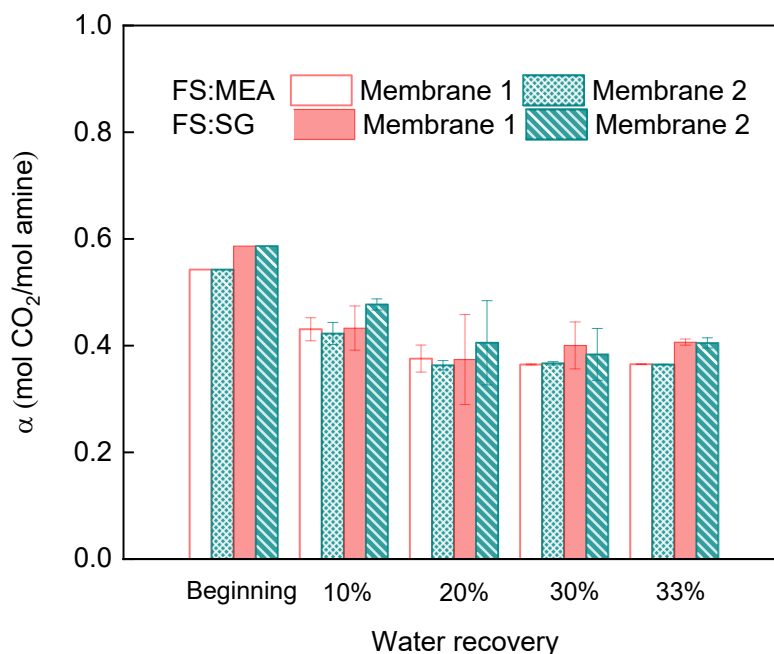
250 **3.1.1 CO₂ loading**

251 The CO₂ loading ratios for MEA and sodium glycinate were 0.54 and 0.59 mol/mol,
252 respectively. These results are consistent with the literature [46-48]. CO₂ desorption by DCMD
253 was quantified by monitoring the CO₂ content of the feed solution. Fig. 2 shows 32.8 and 32.4%
254 CO₂ desorption for MEA using Membrane 1 and 2, respectively. Faster desorption rate is
255 observed for MEA when water recovery was between 0 and 20% and no further desorption was
256 observed when water recovery reached 30%. As a thermally driven process, CO₂ desorption is
257 sensitive to temperature. In the current state of the art MEA-based CO₂ capture process, up to
258 50% CO₂ desorption can be achieved but only at a higher temperature (ca. 120 °C).

259 The changing CO₂ desorption rate could be explained by the decrease in CO₂ partial pressure
260 and solution pH increase. At water recovery below 20%, high CO₂ loading and high CO₂ partial
261 pressure resulted in faster CO₂ release via thermolysis. As the desorption process continued,

262 partial pressure of CO₂ loaded solution decreased, leading to lower CO₂ desorption. CO₂
 263 desorption is pH dependent. At high pH, carbamic acid formed via the reaction between CO₂
 264 and MEA deprotonates to carbamate. The process is reversed when CO₂ is desorbed. As the
 265 solution pH increased due to CO₂ desorption, the desorption rate decreased. The desorption
 266 temperature used in this study was much lower than in the conventional amine-based CO₂
 267 capture process; thus, the impact of CO₂ partial pressure and pH on the rate of desorption was
 268 more significant. In the conventional process, carbamate was still detectable in the solution
 269 after desorption, suggesting that complete regeneration of MEA is impractical [24].

270 CO₂ desorption can be also assessed by examining the corresponding pH value of the amine
 271 solution. In this study, the pH value of CO₂ rich-loaded MEA was 8.5 and pH increased to 10.7
 272 after desorption (for both membranes). The pH of solution after desorption did not reach the
 273 initial value of fresh MEA (12.6), which is consistent with the low desorption efficiency under
 274 current experimental condition. Previous works have reported similar CO₂ desorption (32%)
 275 from a MEA solution compared to this study under atmospheric pressure but at 120 °C or higher
 276 temperature [15, 49]. In practice, 50% desorption efficiency is very desirable but still difficult
 277 to be achieved.



278

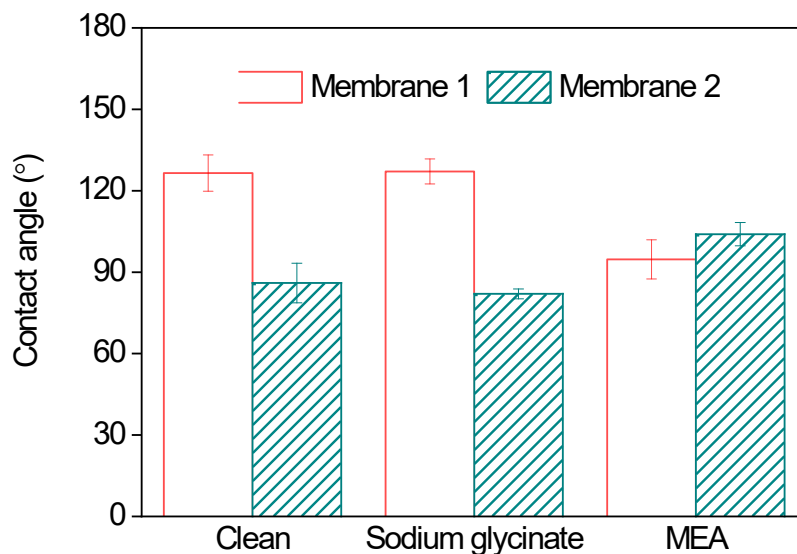
279 Fig. 2. Loading ratio (α) of CO₂ rich-loaded solution by DCMD as a function of water recovery.
 280 Experimental conditions: DI water was used as the distillate. MEA (5 M) and sodium glycinate
 281 (SG, 3 M) were used as the feed. The temperatures of the feed solution and distillate were 80 °C

282 and 25 °C, respectively. All experiments were conducted in duplicate. The error bars represent
283 the difference between two replicate experiments.

284 The decrease in CO₂ loading in the amine solution in Fig. 2 can be used to quantify CO₂
285 desorption. CO₂ desorption from a sodium glycinate solution has a similar profile to that of
286 MEA (Fig. 2). Membrane 1 and 2 showed maximum CO₂ desorption efficiency of 36.3% and
287 34.6%, respectively. CO₂ desorption from MEA solution became negligible when water
288 recovery reached 30%. Similar to MEA, sodium glycinate can also form a stable intermediate
289 via reaction with CO₂ [50]. As water recovery exceeded 20%, no further CO₂ desorption was
290 observed with Membrane 1.

291 3.1.2 Wettability behaviour after 30% water recovery

292 The relative wettability of membrane can be determined by contact angle measurement of the
293 membrane surface. There were negligible changes in hydrophobicity for both membranes after
294 desorption experiment using sodium glycinate as the adsorbent (Fig. 3).



295

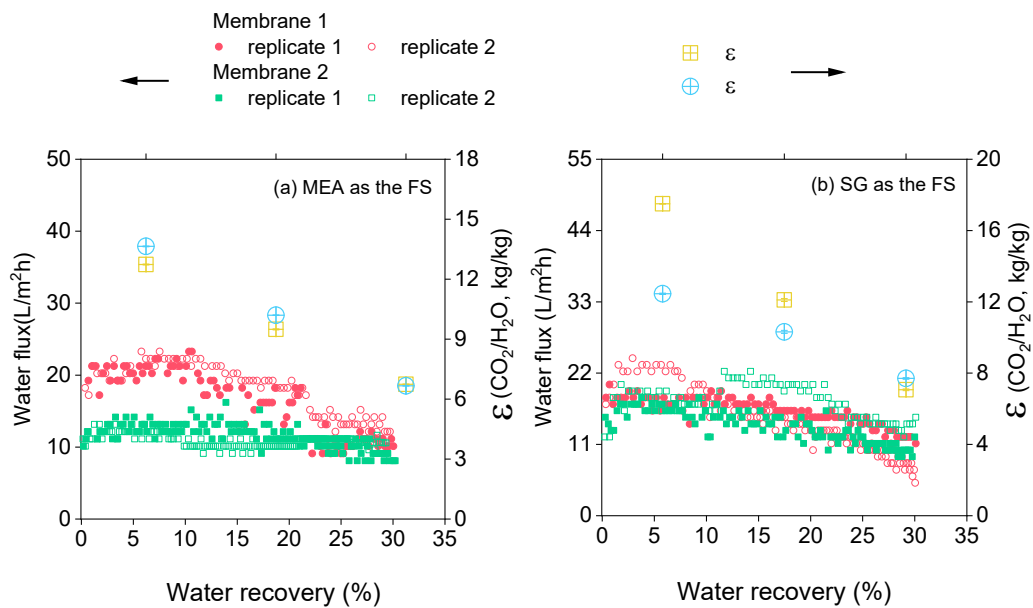
296 Fig. 3. Contact angles of membranes before and after the DCMD process (30% water recovery).
297 Error bars represent the standard deviation of five repetitive measurements.

298 Interaction between MEA and membrane polymer could alter the membrane hydrophobicity
299 [51]; however, changes in the membrane water contact angle were dependent on the initial
300 hydrophobicity. MEA resulted in a decline in water contact angle of Membrane 1 from 127 to
301 95°. By contrast, contact angle of Membrane 2 increased by 31% after the desorption

302 experiment using MEA as CO₂ adsorbent (Fig. 3). This improvement was possibly due to the
 303 initially low contact angle value of the virgin membrane and membrane swelling caused by the
 304 MEA penetration [52]. Despite the variation in water contact angle due to interaction with
 305 amine adsorbent, results in Fig. 3 confirm that a sufficiently hydrophobic condition may still
 306 be possible for MD operation.

307 3.1.3 Water activity reduction by DCMD

308 CO₂ desorption rate can be facilitated by the water reduction in amine solution. Water reduction
 309 is represented by the water production in distillate side in terms of water flux in DCMD. Water
 310 fluxes during the CO₂ desorption experiment when MEA was used as the absorbent are
 311 reported in Fig. 4a. Membrane 1 had an initial flux of 21.2 L/m²·h, which was stable for only
 312 the initial 100 minutes of the desorption experiment. It then declined to 10.1 L/m²·h at the end
 313 of process possibly due to partial membrane wetting. On the other hand, Membrane 2 showed
 314 a more stable water flux throughout the desorption experiment possibly it is thinner and more
 315 porous than Membrane 1 (Table 1).



316

317 Fig. 4. Water flux and ratios of removed CO₂ and condensed water by DCMD during CO₂
 318 desorption using different adsorbent: (a) MEA and (b) SG. Experimental conditions are
 319 described in Fig. 2.

320 Membrane 1 was thicker (Table 1) but also produced a higher initial water flux than Membrane
 321 2. In the DCMD process, a thick membrane resulted in a higher resistance to mass transfer of

322 water vapour but also prevent unnecessary thermal conduction. This observation was also
323 possibly due to the different hydrophobicity between these two membranes (Fig. 3). Membrane
324 hydrophobicity appears to be a determining factor of the water flux trend for DCMD with MEA
325 regeneration.

326 When sodium glycinate was used as the absorbent, both membranes showed a similar and more
327 flux decline compared to MEA (Fig. 4b) despite the difference in their initial hydrophobicity.
328 Exposure to sodium glycinate did not significantly alter the membrane hydrophobicity (Fig. 3).
329 Thus, most of this flux decline observed in Fig 4b can be attributed to the increase in viscosity
330 of the sodium glycinate solution as it becomes more concentrated [53].

331 The stable hydrophobicity of both membranes (section 3.1.2) could prevent the penetration of
332 sodium glycinate through membrane pore into distillate, thus, maintaining high distillate
333 quality. This is consistent with the high solute rejection (>98%) observed for amines in this
334 study (Supplementary data Fig. S2). Given the high rejection of MEA and sodium glycinate by
335 DCMD, amine loss during the CO₂ desorption can be avoided.

336 The ratio of CO₂ removed over water condensed, ϵ , can be considered as an indicator of the
337 energy requirement. In Fig. 4, ϵ declined as a function of water recovery when both amines
338 were used as the feed. Water condensed led to the increasing concentration of amine solution,
339 which constrain the CO₂ desorption. Due to a higher carbamate stability, MEA showed a lower
340 ϵ than sodium glycinate at the same water recovery. Associated with the decreasing CO₂
341 loading, both membranes showed high amine rejection (>98%) (Supplementary data Fig. S2).

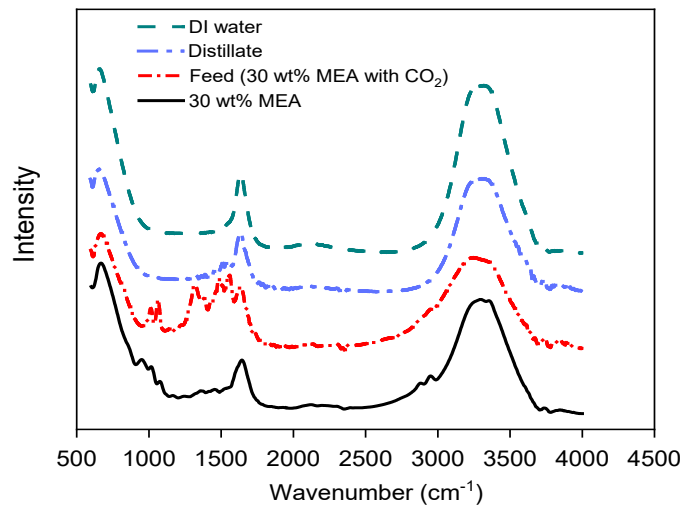
342 3.1.4 Amine loss in the DCMD distillate

343 TOC measurement shows no discernible increase in carbon content of the distillate, indicating
344 no or negligible amine loss to the distillate by the DCMD process (Table 2). FTIR was used to
345 further examine amine loss to the distillate being a reliable analytical technique to monitor the
346 chemical reaction due to the measurable change of a molecule's dipole moment in the mid-IR
347 region (400 - 4000 cm⁻¹). It is to be noted that peaks appearing between 3000 and 4000 cm⁻¹
348 provided information unrelated to chemical reaction between CO₂ and amine. This is because
349 that hydrogen bonding and O-H stretching of H₂O resulted in some broad peaks between 3200
350 and 3700 cm⁻¹. In addition, other chemical bonds (i.e. N-H, C-H, and O-H) stretching also
351 resulted in the particular peaks in this wide region. Thus, this region is known as "the hydrogen
352 stretching region", which is not included in our further discussion.

353 Table 2. Concentration of MEA and sodium glycinate in feed and distillate. Error bars represent
 354 the difference of two replicate measurements.

Membrane	MEA as the feed solution			Sodium glycinate as the feed solution		
	Feed (g/L)	Distillate (g/L)	Rejection (%)	Feed (g/L)	Distillate (g/L)	Rejection (%)
1	43.4 ± 3.5	0.3 ± 0.0	99.3 ± 0.0	18.4 ± 2.8	0.21 ± 0.03	98.9 ± 0.1
2	43.9 ± 5.2	0.8 ± 0.1	98.1 ± 0.2	18.8 ± 1.9	0.10 ± 0.02	99.5 ± 0.1

355 The infrared spectra of aqueous MEA prior to/after CO₂ absorption are given in Fig. 5. Several
 356 characteristic vibration modes appeared prior to CO₂ absorption, for example, C-N-H out-of-
 357 plane bending and C-NH₂ twisting at 950 cm⁻¹, C-O stretching at 1016 cm⁻¹, and C-N stretching
 358 at 1076 cm⁻¹, and N-H rocking at 1645 cm⁻¹ [54]. After molecular CO₂ dissolving into MEA,
 359 several peaks shifted due to the protonation of the MEA and formation of carbamate and
 360 bicarbonate. Specifically, N-COO⁻ stretching vibration was observed at 1319 cm⁻¹. COO⁻
 361 symmetric and asymmetric stretching occurred at 1486 and 1568 cm⁻¹, respectively [54, 55].
 362 As reported by Richner and Puxty [54], the variation in peak intensity was indicated by the
 363 difference of CO₂ loading in aqueous MEA. Shifting peaks was therefore not expected to occur
 364 after desorption.

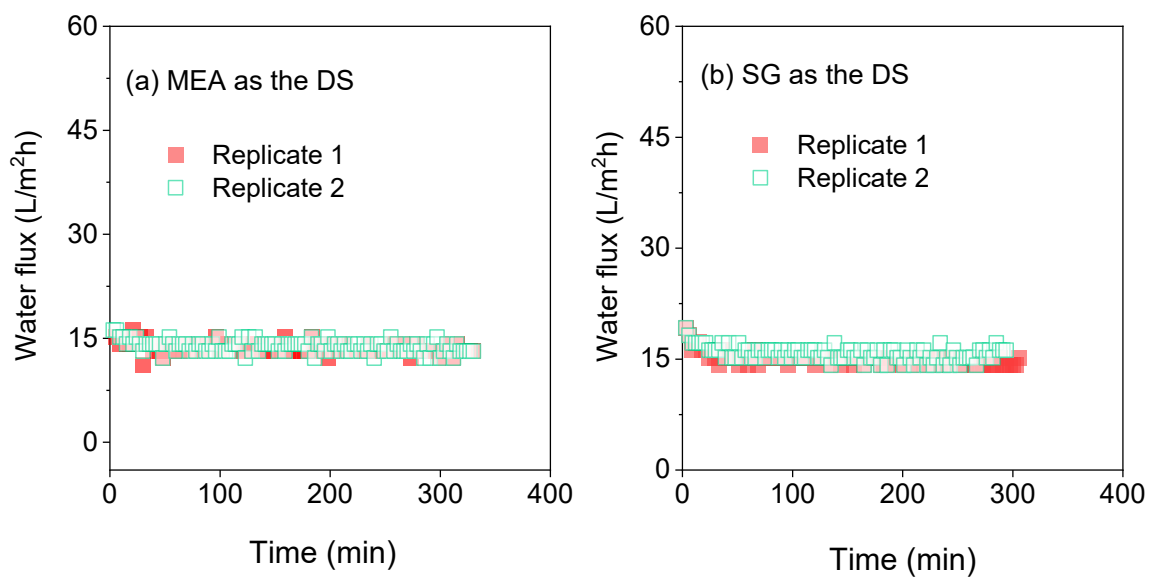


365
 366 Fig. 5. Infrared spectra of the aqueous 30 wt % MEA (black line), feed solution: aqueous MEA
 367 at 0.59 mol/mol CO₂ loading (red line), distillate from the DCMD process (blue line), DI water
 368 as the reference (green line).

369 The infrared spectra of distillate and DI water were compared to validate the high rejection for
370 DCMD (Fig. 5). These results were consistent with data obtained in supplementary data Fig.
371 S2. The spectrum of distillate was identical to that of DI water in spite of several negligible
372 peaks between 1500 and 1568 cm^{-1} . This observation indicated that small amounts of
373 carbamates had penetrated through membrane pore via water vapour. Unlike MEA, sodium
374 glycinate can hardly vaporize as a salt even at a high temperature.

375 3.2 Make-up water by FO

376 The regenerated amines were used as the draw solution to obtain make-up water from
377 secondary treated effluent. The water flux was stable and membrane fouling was not observed
378 when either MEA or sodium glycinate was the draw solution (Fig. 6). It is noteworthy that the
379 initial concentrations of MEA and sodium glycinate for CO_2 adsorption were 5 and 3 M,
380 respectively (section 2.2). Despite this difference in concentration, they resulted in the same
381 water flux of 15 LMH. This is because MEA and sodium glycinate are not ideal electrolytes.
382 As elucidated in a previous study, the osmotic pressure does not increase linearly as the
383 concentration increase and there is a threshold concentration at which the osmotic pressure
384 does not increase any further [42]. This result necessitates further investigation in terms of
385 water flux optimisation. The FO process also provides cooling to the generated amine solution
386 although it is beyond the scope of this current study.



387

388 Fig. 6. Water flux profile of the FO process for regenerated amine solutions versus DI water
389 and treated effluent: (a) MEA at 5M as the draw solution (DS); (b) Sodium glycinate at 3M as

390 the DS. Feed solution (FS) and DS were circulated in the counter-current direction. Replicate
 391 experiments were conducted in AL-DS membrane orientation until 30% water recovery.

392 3.3 Repetitive CO₂ absorption by amine solutions after desorption

393 Table 3: CO₂ loading α from selected amine solutions in the different stage of experiment.

394 Treated effluent and DI water were used as the cooling sources, unit: mol CO₂/mol amine.

Selected Solution	1 st cycle CO ₂ absorption	1 st cycle CO ₂ desorption	Desorption efficiency	2 nd cycle of CO ₂ absorption (after FO)	Re-adsorption efficiency
MEA	0.54	0.36	33.3%	0.47	87.0%
SG	0.59	0.39	33.9%	0.52	88.1%

395 Repetitive CO₂ absorption and desorption performance for both MEA and sodium glycinate by
 396 the MD-FO process is summarised in Table 3. In the first cycle, MEA exhibited the 33.3% CO₂
 397 desorption efficiency with sodium glycinate slightly higher at 33.9%. Due to the high rejection
 398 of FO process (supplementary data Fig. S3), treated effluent could provide adequately clean
 399 water to cool down the heated amine solution for repetitive absorption. MEA and sodium
 400 glycinate also showed similar re-absorption efficiency of 87.0 and 88.1%, respectively. The
 401 observed re-absorption efficiency of below 100% in the 2nd cycle highlight the need for further
 402 investigation since in a practical application, the performance must be stable over thousands of
 403 cycles. It is noteworthy that amine loss from MD desorption was insignificant (section 3.1.4).
 404 Thermal degradation was also expected to be negligible given the low desorption temperature
 405 (~80 °C) in this study.

406 3.4 Future work for practical applications

407 The proposed MD-FO process has shown some initial and promising results for the repetitive
 408 amine-based CO₂ capture from flue gas. Results reported in this study also highlight several
 409 technical challenges for further research and development. Future research work is
 410 recommended to include the screening of other commercially available amine solutions for
 411 CO₂ desorption by the MD system. Their respective CO₂ desorption and degradation are
 412 important parameters to assess their practical applications in the MD system. Further FO
 413 membrane development is recommended to limit the reverse salt flux for low or zero amine
 414 loss and stable water flux during the cooling process. A techno-economic analysis of the
 415 integrated system including the overall energy consumption requirement is also necessary to
 416 evaluate the potential of our proposed MD-FO process for practical applications.

417 **4 Conclusion**

418 This study demonstrated an integrated MD-FO system for the continuous CO₂ capture. MD-
419 FO simultaneously provides low temperature CO₂ desorption and trim cooling as a promising
420 alternative to utilize waste heat and treated effluent in power plants. The MD process achieved
421 33.6 and 33.2% CO₂ desorption efficiency for MEA and sodium glycinate at 80 °C, respectively.
422 Interaction between amine adsorbent and the MD membrane could alter the membrane surface
423 contact angle with water but under all experimental conditions, it was sufficiently hydrophobic
424 for MD operation. Amine loss during CO₂ desorption by MD was insignificant. The
425 regenerated MEA and sodium glycinate exhibited stable FO water flux for make-up water
426 provision when secondary treated effluent was used as the feed. The results also highlight a
427 major technical challenge for further investigation. Repetitive CO₂ loading and desorption
428 showed less than 90% CO₂ re-absorption efficiency for either MEA or sodium glycinate in the
429 second cycle. It is necessary to delineate the reason for this incomplete re-adsorption in a future
430 study. Although this study is still preliminary, it provides important experimental data for
431 further development of a novel membrane-based platform for CO₂ capture from flue gas.

432 **Acknowledgement**

433 The authors thank the financial support from the Australian Research Council through the ARC
434 Research Hub for Energy-efficient Separation (IH170100009). Lei Zheng would like to express
435 his gratitude to Faculty of Engineering and Information Technology (FEIT), University of
436 Technology Sydney (UTS) for awarding him a FEIT PhD Post-Thesis Publication Award. His
437 gratitude also goes to China Scholarship Council and UTS for the provision of a doctoral
438 scholarship. Mr Minh Vu is acknowledged for his help in FTIR analysis.

439 **Reference**

- 440 [1] G.P. Peters, R.M. Andrew, J.G. Canadell, P. Friedlingstein, R.B. Jackson, J.I. Korsbakken, C. Le
441 Quéré, A. Peregon, Carbon dioxide emissions continue to grow amidst slowly emerging climate policies,
442 Nature Climate Change, (2019).
- 443 [2] S. Liu, H. Ling, J. Lv, H. Gao, Y. Na, Z. Liang, New Insights and Assessment of Primary
444 Alkanolamine/Sulfolane Biphasic Solutions for Post-combustion CO₂ Capture: Absorption, Desorption,
445 Phase Separation, and Technological Process, Industrial & Engineering Chemistry Research, 58 (2019)
446 20461-20471.
- 447 [3] K. Xie, Q. Fu, G.G. Qiao, P.A. Webley, Recent progress on fabrication methods of polymeric thin
448 film gas separation membranes for CO₂ capture, Journal of Membrane Science, 572 (2019) 38-60.

449 [4] S. Zhao, P.H.M. Feron, L. Deng, E. Favre, E. Chabanon, S. Yan, J. Hou, V. Chen, H. Qi, Status and
450 progress of membrane contactors in post-combustion carbon capture: A state-of-the-art review of new
451 developments, *Journal of Membrane Science*, 511 (2016) 180-206.

452 [5] P. Luis, T. Van Gerven, B. Van der Bruggen, Recent developments in membrane-based technologies
453 for CO₂ capture, *Progress in Energy and Combustion Science*, 38 (2012) 419-448.

454 [6] K. Li, W. Leigh, P. Feron, H. Yu, M. Tade, Systematic study of aqueous monoethanolamine (MEA)-
455 based CO₂ capture process: Techno-economic assessment of the MEA process and its improvements,
456 *Applied Energy*, 165 (2016) 648-659.

457 [7] Y. Li, L.a. Wang, Z. Tan, Z. Zhang, X. Hu, Experimental studies on carbon dioxide absorption using
458 potassium carbonate solutions with amino acid salts, *Separation and Purification Technology*, 219
459 (2019) 47-54.

460 [8] F. Barzagli, C. Giorgi, F. Mani, M. Peruzzini, Comparative Study of CO₂ Capture by Aqueous and
461 Nonaqueous 2-Amino-2-methyl-1-propanol Based Absorbents Carried Out by ¹³C NMR and Enthalpy
462 Analysis, *Industrial & Engineering Chemistry Research*, 58 (2019) 4364-4373.

463 [9] K. Stéphenne, Start-up of World's First Commercial Post-combustion Coal Fired CCS Project:
464 Contribution of Shell Cansolv to SaskPower Boundary Dam ICCS Project, *Energy Procedia*, 63 (2014)
465 6106-6110.

466 [10] Petra Nova - W.A. Parish Project in, Office of Fossil Energy, 2018.

467 [11] Z. Zhang, Y. Li, W. Zhang, J. Wang, M.R. Soltanian, A.G. Olabi, Effectiveness of amino acid salt
468 solutions in capturing CO₂: A review, *Renewable and Sustainable Energy Reviews*, 98 (2018) 179-188.

469 [12] S. Moioli, L.A. Pellegrini, M.T. Ho, D.E. Wiley, A comparison between amino acid based solvent
470 and traditional amine solvent processes for CO₂ removal, *Chemical Engineering Research and Design*,
471 146 (2019) 509-517.

472 [13] D. Guo, H. Thee, C.Y. Tan, J. Chen, W. Fei, S. Kentish, G.W. Stevens, G. da Silva, Amino Acids
473 as Carbon Capture Solvents: Chemical Kinetics and Mechanism of the Glycine + CO₂ Reaction, *Energy
474 & Fuels*, 27 (2013) 3898-3904.

475 [14] M. Caplow, Kinetics of carbamate formation and breakdown, *Journal of the American Chemical
476 Society*, 90 (1968) 6795-6803.

477 [15] B. Lv, B. Guo, Z. Zhou, G. Jing, Mechanisms of CO₂ Capture into Monoethanolamine Solution
478 with Different CO₂ Loading during the Absorption/Desorption Processes, *Environmental Science &
479 Technology*, 49 (2015) 10728-10735.

480 [16] P. Singh, G.F. Versteeg, Structure and activity relationships for CO₂ regeneration from aqueous
481 amine-based absorbents, *Process Safety and Environmental Protection*, 86 (2008) 347-359.

482 [17] R. Idem, M. Wilson, P. Tontiwachwuthikul, A. Chakma, A. Veawab, A. Aroonwilas, D. Gelowitz,
483 Pilot Plant Studies of the CO₂ Capture Performance of Aqueous MEA and Mixed MEA/MDEA
484 Solvents at the University of Regina CO₂ Capture Technology Development Plant and the Boundary

485 Dam CO₂ Capture Demonstration Plant, *Industrial & Engineering Chemistry Research*, 45 (2006) 2414-
486 2420.

487 [18] G.T. Rochelle, Amine Scrubbing for CO₂ Capture, *Science*, 325 (2009) 1652.

488 [19] S.J. Vevelstad, I. Eide-Haugmo, E.F. da Silva, H.F. Svendsen, Degradation of MEA; a theoretical
489 study, *Energy Procedia*, 4 (2011) 1608-1615.

490 [20] K. Li, P.H.M. Feron, T.W. Jones, K. Jiang, R.D. Bennett, A.F. Hollenkamp, Energy harvesting
491 from amine-based CO₂ capture: proof-of-concept based on mono-ethanolamine, *Fuel*, 263 (2020)
492 116661.

493 [21] S.J. McGurk, C.F. Martín, S. Brandani, M.B. Sweatman, X. Fan, Microwave swing regeneration
494 of aqueous monoethanolamine for post-combustion CO₂ capture, *Applied Energy*, 192 (2017) 126-133.

495 [22] B. Dutcher, M. Fan, A.G. Russell, Amine-Based CO₂ Capture Technology Development from the
496 Beginning of 2013—A Review, *ACS Applied Materials & Interfaces*, 7 (2015) 2137-2148.

497 [23] C.-h. Cheng, K. Li, H. Yu, K. Jiang, J. Chen, P. Feron, Amine-based post-combustion CO₂ capture
498 mediated by metal ions: Advancement of CO₂ desorption using copper ions, *Applied Energy*, 211 (2018)
499 1030-1038.

500 [24] K. Li, P. van der Poel, W. Conway, K. Jiang, G. Puxty, H. Yu, P. Feron, Mechanism Investigation
501 of Advanced Metal–Ion–Mediated Amine Regeneration: A Novel Pathway to Reducing CO₂ Reaction
502 Enthalpy in Amine-Based CO₂ Capture, *Environmental Science & Technology*, 52 (2018) 14538-14546.

503 [25] D.B. Gingerich, M.S. Mauter, Quantity, Quality, and Availability of Waste Heat from United States
504 Thermal Power Generation, *Environmental Science & Technology*, 49 (2015) 8297-8306.

505 [26] P.-H. Lin, D.S.H. Wong, Carbon dioxide capture and regeneration with amine/alcohol/water blends,
506 *International Journal of Greenhouse Gas Control*, 26 (2014) 69-75.

507 [27] Q. Lai, L. Kong, W. Gong, A.G. Russell, M. Fan, Low-energy-consumption and environmentally
508 friendly CO₂ capture via blending alcohols into amine solution, *Applied Energy*, 254 (2019) 113696.

509 [28] E.S. Hamborg, C. van Aken, G.F. Versteeg, The effect of aqueous organic solvents on the
510 dissociation constants and thermodynamic properties of alkanolamines, *Fluid Phase Equilibria*, 291
511 (2010) 32-39.

512 [29] F. Barzagli, F. Mani, M. Peruzzini, Efficient CO₂ absorption and low temperature desorption with
513 non-aqueous solvents based on 2-amino-2-methyl-1-propanol (AMP), *International Journal of*
514 *Greenhouse Gas Control*, 16 (2013) 217-223.

515 [30] F. Barzagli, C. Giorgi, F. Mani, M. Peruzzini, Reversible carbon dioxide capture by aqueous and
516 non-aqueous amine-based absorbents: A comparative analysis carried out by ¹³C NMR spectroscopy,
517 *Applied Energy*, 220 (2018) 208-219.

518 [31] P. Wang, T.-S. Chung, Recent advances in membrane distillation processes: Membrane
519 development, configuration design and application exploring, *Journal of Membrane Science*, 474 (2015)
520 39-56.

521 [32] G. Naidu, L. Tijing, M.A.H. Johir, H. Shon, S. Vigneswaran, Hybrid membrane distillation:
522 Resource, nutrient and energy recovery, *Journal of Membrane Science*, 599 (2020) 117832.

523 [33] W. Jia, J.A. Kharraz, P.J. Choi, J. Guo, B.J. Deka, A.K. An, Superhydrophobic membrane by
524 hierarchically structured PDMS-POSS electro spray coating with cauliflower-shaped beads for
525 enhanced MD performance, *Journal of Membrane Science*, 597 (2020) 117638.

526 [34] S.S. Ray, M. Gandhi, S.-S. Chen, H.-M. Chang, C.T.N. Dan, H.Q. Le, Anti-wetting behaviour of
527 a superhydrophobic octadecyltrimethoxysilane blended PVDF/recycled carbon black composite
528 membrane for enhanced desalination, *Environmental Science: Water Research & Technology*, 4 (2018)
529 1612-1623.

530 [35] Z. Xiao, H. Guo, H. He, Y. Liu, X. Li, Y. Zhang, H. Yin, A.V. Volkov, T. He, Unprecedented
531 scaling/fouling resistance of omniphobic polyvinylidene fluoride membrane with silica nanoparticle
532 coated micropillars in direct contact membrane distillation, *Journal of Membrane Science*, 599 (2020)
533 117819.

534 [36] H.C. Duong, A.R. Chivas, B. Nelemans, M. Duke, S. Gray, T.Y. Cath, L.D. Nghiem, Treatment
535 of RO brine from CSG produced water by spiral-wound air gap membrane distillation — A pilot study,
536 *Desalination*, 366 (2015) 121-129.

537 [37] L. Song, Z. Ma, X. Liao, P.B. Kosaraju, J.R. Irish, K.K. Sirkar, Pilot plant studies of novel
538 membranes and devices for direct contact membrane distillation-based desalination, *Journal of*
539 *Membrane Science*, 323 (2008) 257-270.

540 [38] N.A. Rahim, N. Ghasem, M. Al-Marzouqi, Absorption of CO₂ from natural gas using different
541 amino acid salt solutions and regeneration using hollow fiber membrane contactors, *Journal of Natural*
542 *Gas Science and Engineering*, 26 (2015) 108-117.

543 [39] S. Zhao, C. Cao, L. Wardhaugh, P.H.M. Feron, Membrane evaporation of amine solution for
544 energy saving in post-combustion carbon capture: Performance evaluation, *Journal of Membrane*
545 *Science*, 473 (2015) 274-282.

546 [40] P. Feron, R. Thiruvengkatachari, A. Cousins, Water production through CO₂ capture in coal-fired
547 power plants, *Energy Science & Engineering*, 5 (2017) 244-256.

548 [41] G. Gwak, D.I. Kim, J. Kim, M. Zhan, S. Hong, An integrated system for CO₂ capture and water
549 treatment by forward osmosis driven by an amine-based draw solution, *Journal of Membrane Science*,
550 581 (2019) 9-17.

551 [42] L. Zheng, W.E. Price, T. He, L.D. Nghiem, Simultaneous cooling and provision of make-up water
552 by forward osmosis for post-combustion CO₂ capture, *Desalination*, 476 (2020) 114215.

553 [43] L.N. Nguyen, M.V. Truong, A.Q. Nguyen, M.A.H. Johir, A.S. Commault, P.J. Ralph, G.U.
554 Semblante, L.D. Nghiem, A sequential membrane bioreactor followed by a membrane microalgal
555 reactor for nutrient removal and algal biomass production, *Environmental Science: Water Research &*
556 *Technology*, 6 (2020) 189-196.

557 [44] E.J. Novek, E. Shaulsky, Z.S. Fishman, L.D. Pfefferle, M. Elimelech, Low-Temperature Carbon
558 Capture Using Aqueous Ammonia and Organic Solvents, *Environmental Science & Technology Letters*,
559 3 (2016) 291-296.

560 [45] A. Aroonwilas, P. Tontiwachwuthikul, Mass Transfer Coefficients and Correlation for CO₂
561 Absorption into 2-Amino-2-methyl-1-propanol (AMP) Using Structured Packing, *Industrial &*
562 *Engineering Chemistry Research*, 37 (1998) 569-575.

563 [46] K. Li, A. Cousins, H. Yu, P. Feron, M. Tade, W. Luo, J. Chen, Systematic study of aqueous
564 monoethanolamine-based CO₂ capture process: model development and process improvement, 4 (2016)
565 23-39.

566 [47] X. Zhang, X. Zhang, H. Liu, W. Li, M. Xiao, H. Gao, Z. Liang, Reduction of energy requirement
567 of CO₂ desorption from a rich CO₂-loaded MEA solution by using solid acid catalysts, *Applied Energy*,
568 202 (2017) 673-684.

569 [48] M. Rabensteiner, G. Kinger, M. Koller, G. Gronald, S. Unterberger, C. Hochenauer, Investigation
570 of the suitability of aqueous sodium glycinate as a solvent for post combustion carbon dioxide capture
571 on the basis of pilot plant studies and screening methods, *International Journal of Greenhouse Gas*
572 *Control*, 29 (2014) 1-15.

573 [49] Y. Zhao, Y. Bian, H. Li, H. Guo, S. Shen, J. Han, D. Guo, A Comparative Study of Aqueous
574 Potassium Lysinate and Aqueous Monoethanolamine for Postcombustion CO₂ Capture, *Energy & Fuels*,
575 31 (2017) 14033-14044.

576 [50] H.-J. Song, S. Park, H. Kim, A. Gaur, J.-W. Park, S.-J. Lee, Carbon dioxide absorption
577 characteristics of aqueous amino acid salt solutions, *International Journal of Greenhouse Gas Control*,
578 11 (2012) 64-72.

579 [51] Z. Rezaiyan, P. Keshavarz, M. Khorram, Experimental investigation of the effects of different
580 chemical absorbents on wetting and morphology of poly(vinylidene fluoride) membrane, *Journal of*
581 *Applied Polymer Science*, 134 (2017) 45543.

582 [52] N.A. Ahmad, C.P. Leo, A.L. Ahmad, Amine wetting evaluation on hydrophobic silane modified
583 polyvinylidene fluoride/silicoaluminophosphate zeolite membrane for membrane gas absorption,
584 *Journal of Natural Gas Science and Engineering*, 58 (2018) 115-125.

585 [53] M.S. Shaikh, A.M. Shariff, M.A. Bustam, G. Murshid, Analysis of Physicochemical Properties
586 of Aqueous Sodium Glycinate (SG) Solutions at Low Concentrations from 0.1-2.0 M, *Journal of*
587 *Applied Sciences*, 14 (2014) 1055-1060.

588 [54] G. Richner, G. Puxty, Assessing the Chemical Speciation during CO₂ Absorption by Aqueous
589 Amines Using in Situ FTIR, *Industrial & Engineering Chemistry Research*, 51 (2012) 14317-14324.

590 [55] K. Robinson, A. McCluskey, M.I. Attalla, An FTIR Spectroscopic Study on the Effect of Molecular
591 Structural Variations on the CO₂ Absorption Characteristics of Heterocyclic Amines, *ChemPhysChem*,
592 12 (2011) 1088-1099.

593